PCCP

Accepted Manuscript

ROYAL SOCIETY OF CHEMISTRY

www.rsc.org/pccp

Journal Name

ARTICLE

High-resolution separation of thiolate-protected gold clusters by reversed-phase high-performance liquid chromatography

Received 00th January 20xx,
Accepted 00th January 20xx

DOI: 10.1039/x0xx00000x

www.rsc.org/

Yoshiki Niihori,[a] Chihiro Uchida,[a] Wataru Kurashige[a] and Yuichi Negishi*[abc]

Thiolate (RS)-protected gold clusters ($Au_n(SR)_m$) have attracted much attention as building blocks of functional nanomaterials. Our group has been studying the high-resolution separation of $Au_n(SR)_m$ clusters using reversed-phase high-performance liquid chromatography. In this perspective, we summarize our recent results on the separation of $Au_n(SR)_m$ clusters and their doped clusters according to the core size, charge state, ligand composition, and coordination isomer. Additionally, this perspective describes new findings obtained by using high-resolution separation and future prospects for the separation of such types of metal clusters. We believe that the techniques and knowledge gained in this studies would contribute to the creation of $Au_n(SR)_m$ clusters with the desired functions and associated functional nanomaterials.

1. Introduction

A size of a nanoscale is considered to be the smallest size in which materials feature functional properties.[1] Therefore, the development of techniques to process or synthesize materials in a size range of a nanoscale has attracted much attention from the viewpoints of decreasing the size of functional materials, and thereby decreasing the required amounts of valuable resources involved in material fabrication. Traditionally, the top-down technology, as represented by the micromachining of silicon, is used to reduce the size of functional materials. However, smaller functional materials can be created when the materials are assembled from atoms and molecules. Consequently, such bottom-up technology has recently received increasing attention.[2,3]

Thiolate (RS)-protected gold clusters ($Au_n(SR)_m$)[4-45] are nanomaterials synthesized by the bottom–up approach. These clusters exhibit high stability both in solution and solid state. Additionally, they exhibit physical and chemical properties, such as photoluminescence,[5,7,10,46–67] catalytic activity,[9,45,64,68,69] and redox behaviors,[7,27,70] which are not observed in bulk Au. Such properties depend on the size of the metal core (i.e., the number of constituent atoms of the metal core)[46,48] and the type of ligand surrounding the metal core.[55] Owing to these characteristics, $Au_n(SR)_m$ clusters are generating great interest as potential structural units of functional nanomaterials.

In general, these clusters are prepared by reducing Au ions in the presence of thiol in solution.[4,71] Such a method typically produces clusters having a distribution in the core size.[46] However, to achieve controlled physical and chemical properties, the development of techniques for preparing $Au_n(SR)_m$ clusters with atomic precision is essential. Previous studies established various separation methods, such as precipitation,[72] polyacrylamide gel

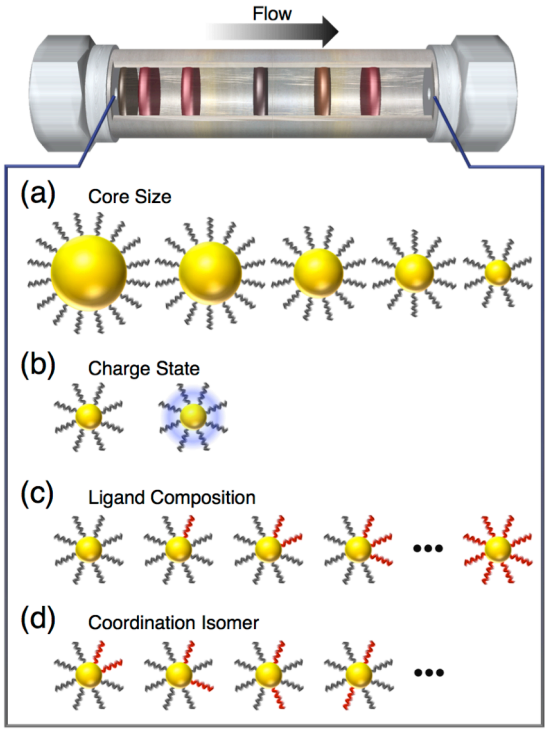

Fig. 1 High-resolution separation of $Au_n(SR)_m$ clusters based on the core size, charge state, ligand composition, and coordination isomer using RP-HPLC.

[a] *Department of Applied Chemistry, Faculty of Science, Tokyo University of Science, 1-3 Kagurazaka, Shinjuku-ku, Tokyo 162-8601, Japan. E-mail: negishi@rs.kagu.tus.ac.jp; Tel: +81-3-5228-9145; Fax: +81-3-5261-4631*
[b] *Photocatalysis International Research Center, Tokyo University of Science, 2641 Yamazaki, Noda, Chiba 278-8510, Japan.*
[c] *Department of Materials Molecular Science, Institute for Molecular Science, Myodaiji, Okazaki, Aichi 444–8585, Japan.*

Table 1. Experimental conditions used in RP-HPLC separation

Separation	Stationary phase	Gradient	Mobile phase	yield (mg) [a]
core size	C8 column [b] + phenyl column [c]	isocratic	10 mM $TBAClO_4$ dichloromethane solution	1.0-5.0
charge state	C8 column [d] + phenyl column [e]	isocratic	10 mM $TBAClO_4$ dichloromethane solution	~0.1
ligand composition	C18 column [f]	linear	methanol → tetrahydrofuran	~0.01
coordination isomer	C18 column [f]	linear	acetonitrile → acetone	~0.01
core size (hydrophilic clusters)	C18 column [f]	linear	25 mM sodium phosphate buffer solution (pH 6.9) → 25 mM $TBAClO_4$ methanol solution	0.01-0.05

[a] Weight of each fraction separated by RP-HPLC. [b] BDS Hypersil C8 column (length × inner diameter: 250 mm × 21.1 mm) with 5 μm particles. [c] BDS Hypersil phenyl column (length × inner diameter: 150 mm × 21.1 mm) with 5 μm particles. [d] BDS Hypersil C8 column (length × inner diameter: 250 mm × 4.6 mm) with 5 μm particles. [e] BDS Hypersil phenyl column (length × inner diameter: 150 mm × 4.6 mm) with 5 μm particles. [f] Hypersil gold column (length × inner diameter: 250 mm × 4.6 mm) with 5 μm particles.

electrophoresis (PAGE),[46,48,73,74] high-performance liquid chromatography (HPLC),[75,76] and solvent extraction,[77–79] which enabled the isolation of $Au_n(SR)_m$ clusters with atomic precision. Recent studies further established the several methods to synthesize only one chemical composition cluster by focusing the prepared clusters into single-sized $Au_n(SR)_m$ clusters[60,80-86] and transforming one stable cluster into another stable cluster.[87-92] This progress enabled the size-selective synthesis of specific types of $Au_n(SR)_m$ clusters. However, at present, a size-selective synthesizing method has only been established for limited types of $Au_n(SR)_m$ clusters. Thus, separation of the resulting mixture of clusters remains an indispensable process to precisely synthesize $Au_n(SR)_m$ clusters. Also, controlling the surrounding ligands is a useful method to create $Au_n(SR)_m$ clusters with specific desired properties. However, except in a limited number of cases, the synthesis of clusters with multiple types of ligands results in a distribution of ligand chemical compositions, and therefore the separation of the $Au_n(SR)_m$ clusters depending on the ligand composition is essential to achieve precise control of the ligand composition.[93–97]

Our group has been studying the high-resolution separation of $Au_n(SR)_m$ clusters and their doped clusters (Fig. 1). Through such studies, we aim to contribute to the improvement of the bottom-up technology in the fabrication of functional nanomaterials. For the separation method, we have focused on reversed-phase high-performance liquid chromatography (RP-HPLC; Fig. 1) which is known to achieve high-resolution separation of organic molecules.[98,99] RP-HPLC has been already employed for the separation of $Au_n(SR)_m$ clusters by Murray and co-workers[75] and Choi and co-workers[76] prior to our study. We have read their literatures, and felt that this type of clusters could be separated with higher resolution under the proper conditions, and then attempted to separate this type of metal clusters by RP-HPLC. The results and progress made in the past 6 years in our study are summarized in this perspective.

2. Separation depending on the core size

The physical and chemical properties of $Au_n(SR)_m$ clusters depend on the number of the constituent atoms. Therefore, it is necessary to separate $Au_n(SR)_m$ clusters depending on the number of constituent atoms with high resolution to obtain $Au_n(SR)_m$ clusters with controlled physical and chemical properties. We have

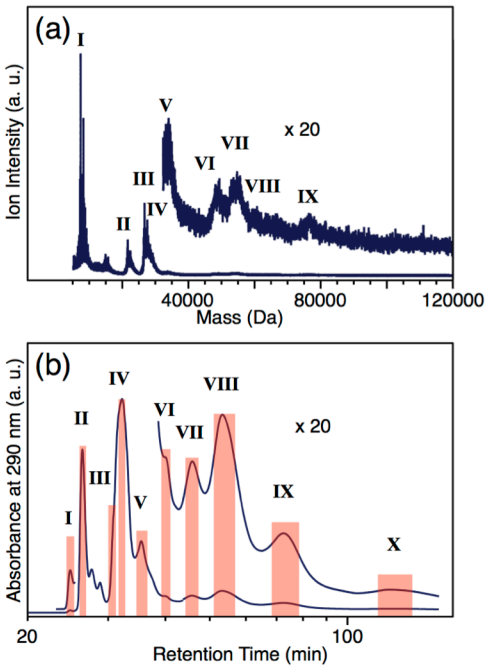

Fig. 2 (a) Positive ion LDI mass spectrum and (b) chromatogram of crude sample of $Au_n(SC_{12}H_{25})_m$ clusters. Adapted from ref. 101.

attempted such separation for dodecanethiolate ($SC_{12}H_{25}$)-protected gold clusters ($Au_n(SC_{12}H_{25})_m$),[100,101] as detailed below.

$Au_n(SC_{12}H_{25})_m$ clusters were prepared using the Brust method.[4] Then, an excessive amount of $C_{12}H_{25}SH$ was added to the prepared clusters, and the mixture was heated at 80°C for 24 h. This process converted the produced clusters into clusters with a limited number of stable species. Then, the most abundant cluster, $Au_{25}(SC_{12}H_{25})_{18}$, in the product was removed by solvent extraction. Fig. 2a shows the laser desorption ionization (LDI) mass spectrum of the product. Multiple peaks were observed in the mass spectrum, indicating that the product contained multiple stable species.[101]

Subsequently, the mixture was separated by RP-HPLC. A dual column setup comprising a C8 column and a phenyl column was used (Table 1). Dichloromethane (CH_2Cl_2) containing

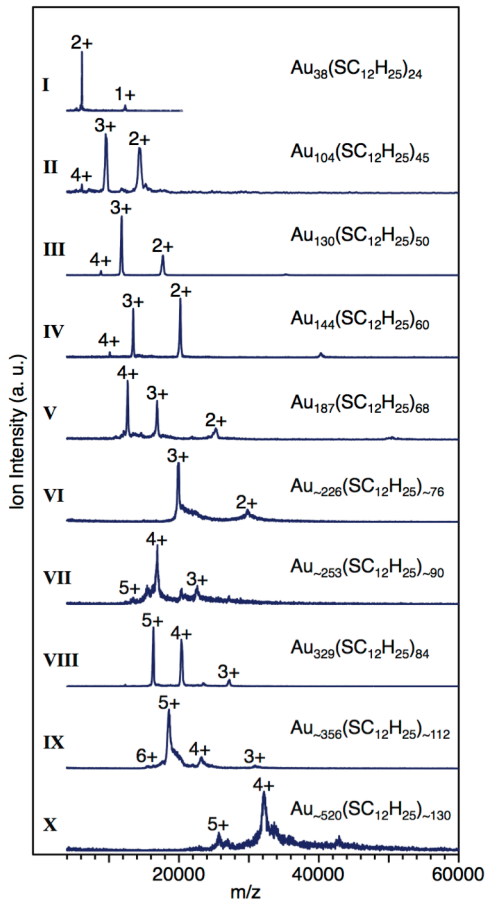

Fig. 3 Positive ion ESI mass spectra of fractions I–X. Adapted from ref. 101.

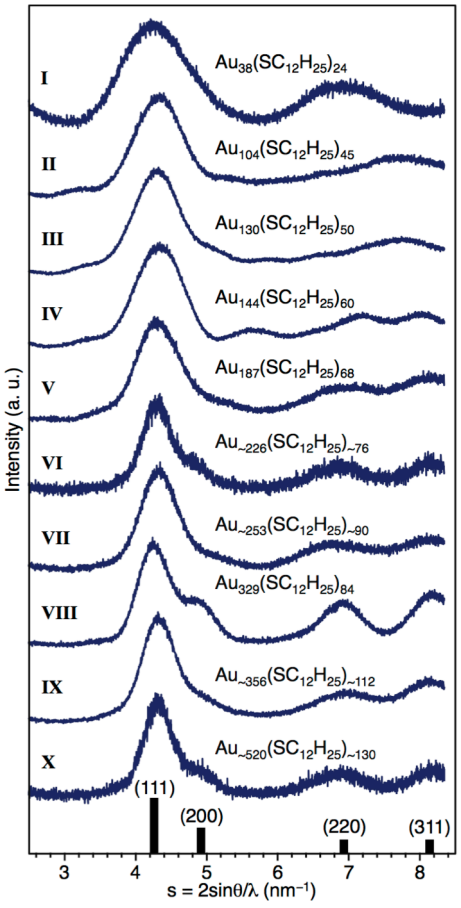

Fig. 4 Powder XRD patterns of fractions I–X. The black vertical bars indicate the peak positions of bulk Au. Adapted from ref. 101.

tetrabutylammonium perchlorate ($TBAClO_4$) (10 mM), was used as the mobile phase solvent (Table 1).[100,101] Fig. 2b shows the obtained chromatogram, which featured multiple peaks. Each peak was fractionated and analyzed by electrospray ionization (ESI) mass spectrometry. The peaks could be assigned to $Au_{38}(SC_{12}H_{25})_{24}$, $Au_{104}(SC_{12}H_{25})_{45}$, $Au_{130}(SC_{12}H_{25})_{50}$, $Au_{144}(SC_{12}H_{25})_{60}$, $Au_{187}(SC_{12}H_{25})_{68}$, $Au_{\sim226}(SC_{12}H_{25})_{\sim76}$, $Au_{\sim253}(SC_{12}H_{25})_{\sim90}$, $Au_{329}(SC_{12}H_{25})_{84}$, $Au_{\sim356}(SC_{12}H_{25})_{\sim112}$, or $Au_{\sim520}(SC_{12}H_{25})_{\sim130}$ with high purity (Fig. 3). These results showed that the $Au_n(SC_{12}H_{25})_m$ clusters were separated according to the number of constituent atoms with high resolution.[101]

The optical absorption spectra of the isolated clusters, measured by Tsukuda and co-workers, revealed the transformation of the electronic structures in the $Au_n(SC_{12}H_{25})_m$ clusters.[101] Peak structures appeared within the near-infrared-to-ultraviolet region for clusters ranging between $Au_{38}(SC_{12}H_{25})_{24}$ and $Au_{144}(SC_{12}H_{25})_{60}$.[101] These peaks became sharper as the temperature decreased. This phenomenon had been reported by Ramakrishna and co-workers and Weissker and co-workers for $Au_n(SR)_m$ clusters featuring discrete electronic structures.[102–104] In contrast, clusters ranging between $Au_{187}(SC_{12}H_{25})_{68}$ and $Au_{\sim520}(SC_{12}H_{25})_{\sim130}$ displayed a distinct peak within the region of 520–540 nm that was attributed to localized surface plasmon resonance (LSPR) effect. The intensity and position of the LSPR band did not change appreciably even at 25 K. These results demonstrated that the clusters ranging from $Au_{187}(SC_{12}H_{25})_{68}$ to $Au_{\sim520}(SC_{12}H_{25})_{\sim130}$ no longer had discrete electronic structures. Based on these results, it was concluded that the transition of electronic structures occurs between $Au_{144}(SC_{12}H_{25})_{60}$ and $Au_{187}(SC_{12}H_{25})_{68}$.[101]

The study conducted on a series of isolated clusters also revealed the transition in the geometrical structures of $Au_n(SC_{12}H_{25})_m$ clusters.[101] Fig. 4 shows the X-ray diffraction (XRD) patterns of the series of isolated $Au_n(SC_{12}H_{25})_m$ clusters. The peaks observed for clusters in the range of $Au_{38}(SC_{12}H_{25})_{24}$ to $Au_{144}(SC_{12}H_{25})_{60}$ did not coincide with those observed for bulk Au. This result implied that these $Au_n(SC_{12}H_{25})_m$ clusters have a different basic structure from bulk Au, which has a face-centered cubic (fcc) structure. Actually, $Au_{38}(SR)_{24}$ has been revealed by single-crystal X-ray structural analysis to have a metal core based on the icosahedral (Ic) structure.[105] The XRD patterns of $Au_{104}(SC_{12}H_{25})_{45}$, $Au_{130}(SC_{12}H_{25})_{50}$, and $Au_{144}(SC_{12}H_{25})_{60}$ were consistent with those calculated by Häkkinen and co-workers of clusters having a metal

core based on the Marks Decahedral (M-Dh) ($Au_{104}(SH)_{45}$), M-Dh ($Au_{130}(SH)_{45}$), and Ic ($Au_{144}(SH)_{60}$) structures, respectively.[101] In contrast, the XRD patterns of clusters ranging from $Au_{187}(SC_{12}H_{25})_{68}$ to $Au_{\sim 520}(SC_{12}H_{25})_{\sim 130}$ displayed peaks at similar positions to those of bulk Au. This result implied that the clusters with these compositions have a fcc structure similar to bulk Au. The XRD patterns of the clusters with this composition range were consistent with the XRD patterns calculated by Häkkinen and co-workers of the $Au_n(SC_{12}H_{25})_m$ clusters possessing a metal core of a fcc structure.[101] Based on these results, it was concluded that in $Au_n(SC_{12}H_{25})_m$ clusters, a transition from bulk to non-bulk, as well as a change in the geometrical structure, occurs within a cluster composition range of $Au_{187}(SC_{12}H_{25})_{68}$ to $Au_{144}(SC_{12}H_{25})_{60}$.[101]

3. Separation depending on the charge state

As shown in Section 2, each $Au_n(SC_{12}H_{25})_m$ cluster displayed different retention times depending on the core size in the RP-HPLC chromatogram. As reported, the relative solubility of $Au_n(SC_{12}H_{25})_m$ clusters in polar solvents decreases with increasing core sizes.[72,78,79,106–108] Thus, it can be considered that the interaction between the $Au_n(SC_{12}H_{25})_m$ clusters and the stationary phase becomes stronger with increasing core sizes, thus resulting in longer retention times (Fig. 2a). Similarly, the solubility of $Au_n(SR)_m$ clusters varies depending on the charge state. For example, neutral $[Au_{25}(SC_6H_{13})_{18}]^0$ exhibits a lower solubility in polar solvents than anionic $[Au_{25}(SC_6H_{13})_{18}]^-$.[78] Accordingly, these two $Au_{25}(SR)_{18}$ clusters, with different charge states, showed different retention times in the RP-HPLC chromatogram, as discussed below.[109,110]

In this study, $[Au_{25}(SC_{12}H_{25})_{18}]^-$ and $[Au_{25}(SC_{12}H_{25})_{18}]^0$ were first synthesized and then their chromatograms were measured. A dual column setup comprising a C8 column and a phenyl column (Table 1) was used as the column and a 10 mM $TBAClO_4$ CH_2Cl_2 solution was used as the mobile phase solvent (Table 1).

Fig. 5a, b shows the chromatograms of $[Au_{25}(SC_{12}H_{25})_{18}]^-$ and $[Au_{25}(SC_{12}H_{25})_{18}]^0$, respectively.[109] $[Au_{25}(SC_{12}H_{25})_{18}]^-$ displayed a peak at a retention time of 10.6 min, whereas $[Au_{25}(SC_{12}H_{25})_{18}]^0$ displayed a peak at a longer retention time of 11.9 min. It can be considered that $[Au_{25}(SC_{12}H_{25})_{18}]^0$ features stronger interactions with the stationary phase when compared with $[Au_{25}(SC_{12}H_{25})_{18}]^-$ because of the lower solubility of the former cluster in polar solvents, thus resulting in a longer retention time. These results implies that $Au_n(SR)_m$ clusters with different charge states can be separated with high resolution by RP-HPLC. In addition, Fig. 5 also shows that the charge state of this type of metal clusters can be estimated by RP-HPLC. Actually, the charge states of $[Au_{24}Pd(SC_{12}H_{25})_{18}]^0$ and $[Au_{25-n}Ag_n(SC_{12}H_{25})_{18}]^-$ (n = 1-11) (Fig. 5c), in which $Au_{25}(SC_{12}H_{25})_{18}$ is doped with Pd or Ag, have been revealed by this experiment.[109,110] It is expected that RP-HPLC will also be widely used in the future for estimating and controlling the charge state of this type of metal clusters.

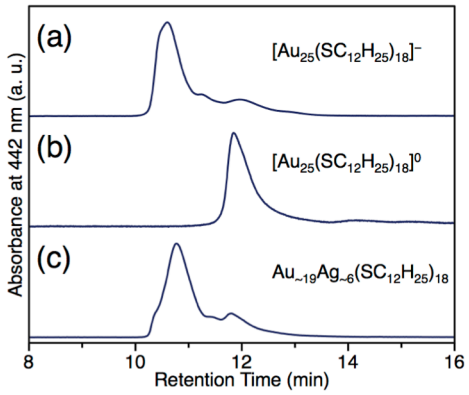

Fig. 5 Chromatograms of (a) $[Au_{25}(SC_{12}H_{25})_{18}]^-$, (b) $[Au_{25}(SC_{12}H_{25})_{18}]^0$, and (c) $Au_{\sim 19}Ag_{\sim 6}(SC_{12}H_{25})_{18}$. Adapted from ref. 109.

4. Separation depending on the ligand composition

The physical and chemical properties of $Au_n(SR)_m$ clusters also depend on the ligands surrounding the metal core. For example, the solubilities and photoluminescence quantum yields[55] of $Au_n(SR)_m$ clusters vary depending on the thiolate functional group. Moreover, the use of a thiolate with a specific functionality as the ligand endows $Au_n(SR)_m$ clusters with functions such as molecular recognition or catalytic abilities.[111] Thus, controlling the ligand composition is an effective way of controlling the cluster functionality. If we can obtain the desired ligand composition, the functions of the resulting clusters can be finely tuned and the arrangement of clusters in certain patterns can also be achieved. Accordingly, we attempted to establish a method to separate this type of metal clusters depending on ligand composition together with the Pradeep group.

We first describe the results obtained for the separation of $Au_{24}Pd$ clusters[110,112–114] protected with $SC_{12}H_{25}$ and 4-*tert*-butyl phenylmethanethiolate (SCH_2Ph^tBu) ($Au_{24}Pd(SC_{12}H_{25})_{18-x}(SCH_2Ph^tBu)_x$).[115] These clusters were synthesized by reacting $Au_{24}Pd(SC_{12}H_{25})_{18}$ (Fig. 6) with 4-*tert*-butyl phenylmethanethiol ($^tBuPhCH_2SH$) at a concentration ratio of $[^tBuPhCH_2SH]/[Au_{24}Pd(SC_{12}H_{25})_{18}]$ = 1000 in CH_2Cl_2 (ligand exchange reaction[116–120]). Fig. 7 shows the matrix-assisted laser desorption ionization (MALDI) mass spectrum of $Au_{24}Pd(SC_{12}H_{25})_{18-x}(SCH_2Ph^tBu)_x$ formed after 2 h of reaction. All of the peaks observed in the mass spectrum were assigned to a series of $Au_{24}Pd(SC_{12}H_{25})_{18-x}(SCH_2Ph^tBu)_x$ (x = 6–16) clusters. This means that the obtained clusters had a distribution in the ligand compositions.[115]

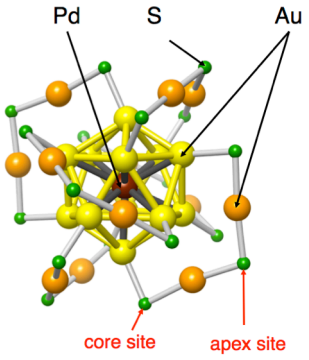

Fig. 6 Geometrical structure determined for $Au_{24}Pd(SR)_{18}$ (refs. 110, 112, and 113). The R groups are omitted for simplicity. Two sites of sulfur (S) discussed in this manuscript are shown in this figure. Adapted from ref. 114.

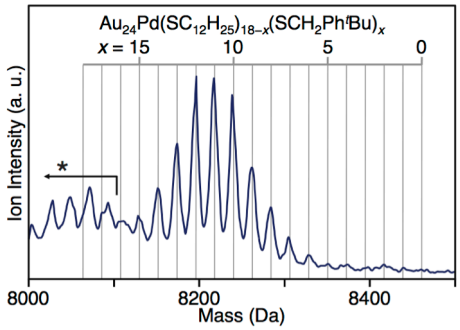

Fig. 7 Negative ion MALDI mass spectrum of $Au_{24}Pd(SC_{12}H_{25})_{18-x}(SCH_2Ph^tBu)_x$ with x = 6–16. The asterisk indicates laser-induced fragments.[107] Adapted from ref. 115.

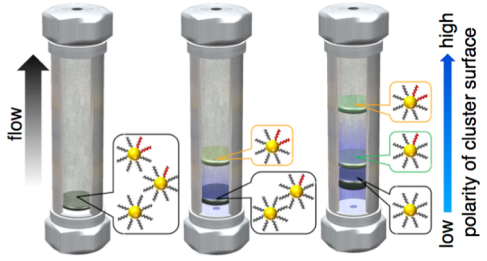

Fig. 8 Schematic of high-resolution separation of metal clusters containing two different types of ligands by RP-HPLC involving mobile phase gradient.

The mixture was then separated by RP-HPLC. A C18 column was used for this separation (Table 1). The products were first adsorbed onto the stationary phase by injecting a suspension of clusters into the column in which a solvent incapable of dissolving the clusters (adsorption solvent) was used as mobile phase (Fig. 8). Then, the products were eluted from the stationary phase in order of cluster surface polarity by gradually introducing a solvent capable of dissolving the clusters (elution solvent) into the mobile phase using a linear gradient program (Fig. 8). Methanol and tetrahydrofuran

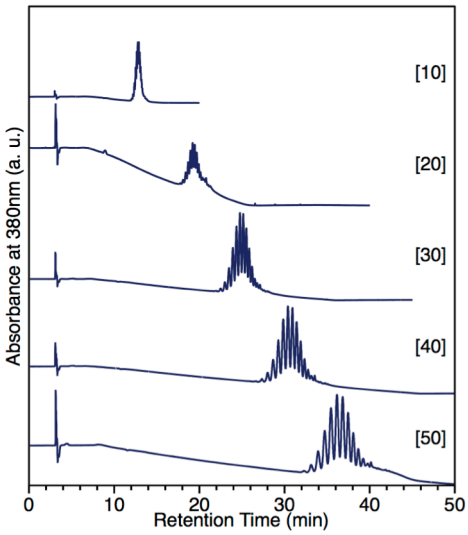

Fig. 9 Chromatograms of $Au_{24}Pd(SC_{12}H_{25})_{18-x}(SCH_2Ph^tBu)_x$ (x = 6–16) at each gradient program. Curve labels (*e.g.*, [10]) indicate the time (in min) taken to replace the mobile phase with THF. The peak observed at 3 min corresponds to the solvent used (THF). Adapted from ref. 115.

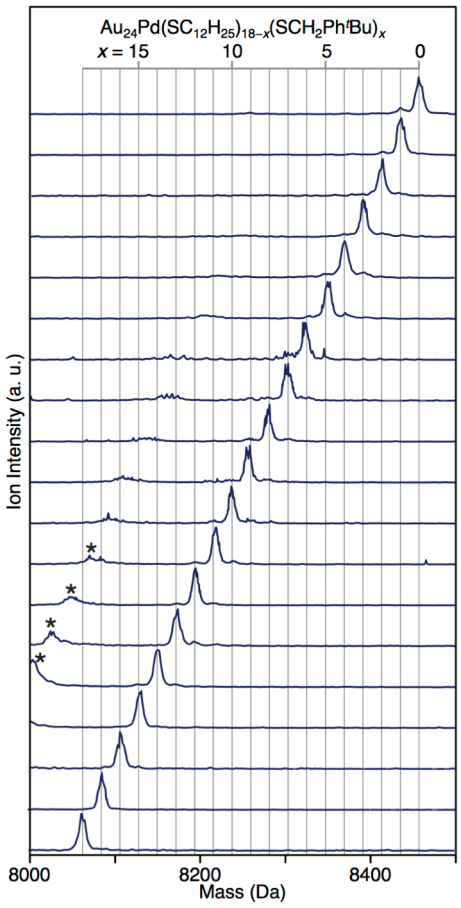

Fig. 10 Negative ion MALDI mass spectra of $Au_{24}Pd(SC_{12}H_{25})_{18-x}(SCH_2Ph^tBu)_x$ (x = 0–18) clusters. Asterisks indicate laser-induced fragments. Adapted from ref. 115.

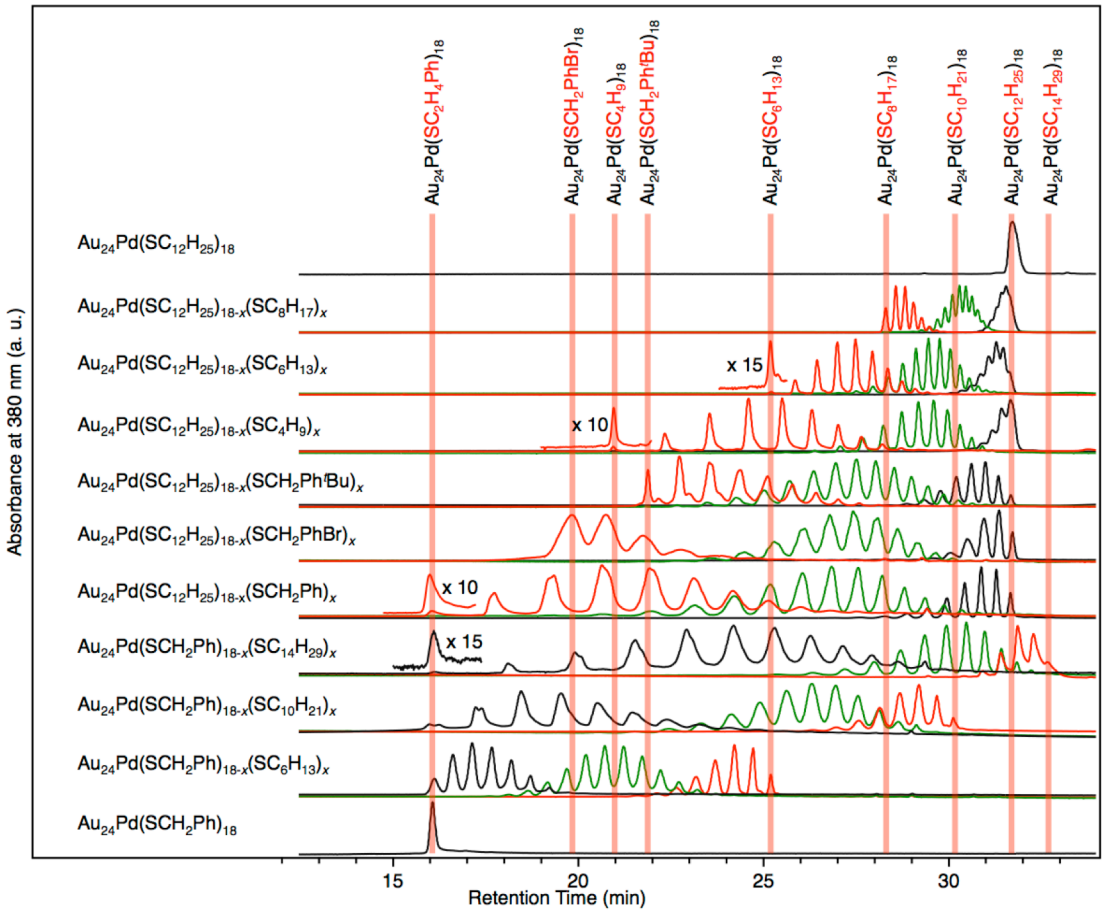

Fig. 11 Chromatograms obtained for $Au_{24}Pd(SR_1)_{18-x}(SR_2)_x$ (x = 0–18) clusters with various ligand combinations (SR_1, SR_2), and $Au_{24}Pd(SC_{12}H_{25})_{18}$ and $Au_{24}Pd(SC_2H_4Ph)_{18}$ for comparison purposes. The MALDI mass spectrum of each $Au_{24}Pd(SR_1)_{18-x}(SR_2)_x$ is provided in ref. 121. In the chromatograms and MALDI mass spectra (ref. 121), the same color indicates the same sample; whereby samples with small, intermediate, and large values of x are represented by the black, green, and red lines, respectively (ref. 121). The orange vertical lines indicate the retention times estimated for $Au_{24}Pd$ clusters protected with one type of ligand *i.e.*, $Au_{24}Pd(SR_1)_{18}$ and $Au_{24}Pd(SR_2)_{18}$. Adapted from ref. 121.

(THF) were used as the adsorption and elution solvents, respectively (Table 1).[115]

Fig. 9 shows the dependence of the chromatograms of $Au_{24}Pd(SC_{12}H_{25})_{18-x}(SCH_2Ph^tBu)_x$ on the time taken to fully replace the mobile phase. When the replacement time was set at 40 min or longer, the peak became more resolved, and the peak distribution looked similar to that of the corresponding MALDI mass spectrum (Fig. 9). Fractionation of each peak followed by mass spectrometry analysis revealed that each peak contained clusters with only one chemical composition. Similar separation/fractionation experiments were performed on $Au_{24}Pd(SC_{12}H_{25})_{18-x}(SCH_2Ph^tBu)_x$ with various ligand distributions. Fig. 10 shows the MALDI mass spectra of the 19 fractions obtained. All mass spectra featured peaks that could be assigned to clusters with one single chemical composition. These results showed that all ligand compositions of $Au_{24}Pd(SC_{12}H_{25})_{18-x}(SCH_2Ph^tBu)_x$ (x = 0–18) could be isolated with high purity by RP-HPLC.[115]

To investigate the versatility of this separation method, similar experiments were conducted using $Au_{24}Pd$ clusters with a combination of other ligands.[121] Fig. 11 shows the chromatograms of $Au_{24}Pd(SR_1)_{18-x}(SR_2)_x$ (x = 0–18) prepared with other ligand combinations (SR_1, SR_2). All chromatograms showed well-resolved and relatively intense peak profiles. The distribution of the peaks in each individual chromatogram was similar to the peak distribution observed in the MALDI mass spectra of the corresponding clusters.[121] These results indicate that this method could be used to separate the $Au_{24}Pd(SR_1)_{18-x}(SR_2)_x$ clusters of Fig. 11 with high resolution. The peaks on the peripheries of the chromatograms obtained from the $Au_{24}Pd(SR_1)_{18-x}(SR_2)_x$ clusters originated from $Au_{24}Pd(SR_1)_{18}$ and $Au_{24}Pd(SR_2)_{18}$. Fig. 11 shows that the polarity of the functional group decreased in the following order: C_2H_4Ph < CH_2PhBr < C_4H_9 < CH_2Ph^tBu < C_6H_{13} < C_8H_{17} < $C_{10}H_{21}$ < $C_{12}H_{25}$ < $C_{14}H_{29}$. In general, the resolution of each chromatogram increased with increasing differences in the polarity of the functional groups of the two types of thiolate ligands (Fig. 11). These results clearly showed

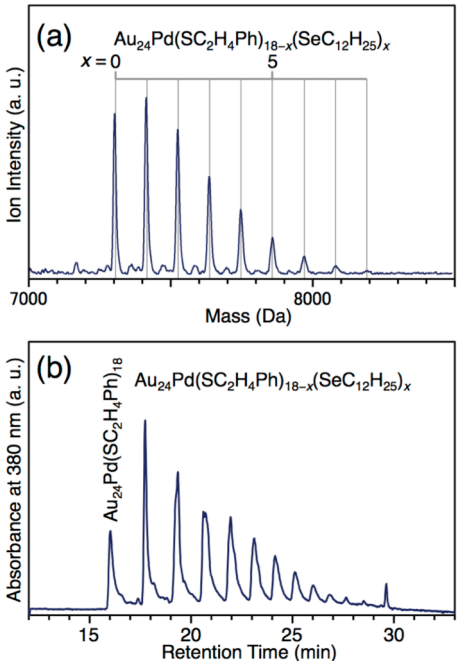

Fig. 12 (a) Negative ion MALDI mass spectrum and (b) chromatogram of $Au_{24}Pd(SC_2H_4Ph)_{18-x}(SeC_{12}H_{25})_x$ (x = 0–8). In (b), the leftmost peak is assigned to $Au_{24}Pd(SC_2H_4Ph)_{18}$ (Fig. 11). Adapted from ref. 121.

that to achieve high-resolution separation of $Au_{24}Pd(SR_1)_{18-x}(SR_2)_x$ clusters, it is essential to increase the difference in the polarity of the functional groups in the two different ligands.

When a suitable combination of functional groups was employed, $Au_{24}Pd(SR_1)_{18-x}(SeR_2)_x$ clusters, in which SR and SeR were used as the two different types of ligands, could also be separated with high resolution (Fig. 12).[121] Thus, this method could afford control over the relative proportions of SR_1 and SeR_2 ligands in the clusters. It has been revealed that charge transfer in the Au–SeR and Au–SR bonds is different, and thus the electron densities of Au in $Au_n(SeR)_m$ and $Au_n(SR)_m$ are different.[122,123] These results showed that this method afforded fine separation of clusters featuring different electron densities of Au. When appropriate ligands were combined, a similar high-resolution separation was achieved for Au_{25} and Au_{38} clusters (Fig. 13).[115] These results indicate that this method is effective regardless of the size or composition of the metal core.

5. Separation depending on the coordination isomer

The $Au_{24}Pd(SR)_{18}$ cluster discussed in the previous section has a geometric structure in which six [–S(R)–Au–S(R)–Au–S(R)–] staples surround the $Au_{12}Pd$ metal core (Fig. 6). Two types of SR units exist in such a geometric structure, namely, SR that is bound directly to the metal core (core site) and SR that is positioned at the center of

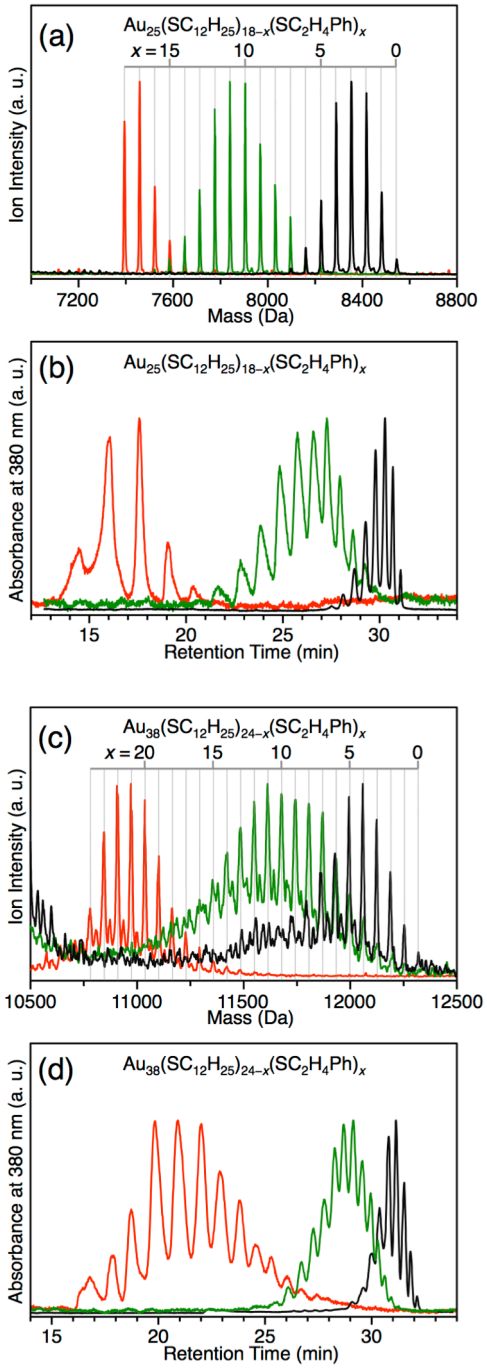

Fig. 13 Comparison between the MALDI mass spectra and chromatograms of (a), (b) $Au_{25}(SC_{12}H_{25})_{18-x}(SC_2H_4Ph)_x$ and (c), (d) $Au_{38}(SC_{12}H_{25})_{24-x}(SC_2H_4Ph)_x$. The MALDI mass spectra in (a) and (c) were observed in negative and positive ion modes, respectively. The same samples in (a), (b), and (c), (d) are indicated by a specific color. In (c), peaks not assigned to $Au_{38}(SC_{12}H_{25})_{24-x}(SC_2H_4Ph)_x$ occur because of laser-induced fragments. Adapted from ref. 115.

the staple (apex site) (Fig. 6). Thus, two coordination isomers[124] can be considered for $Au_{24}Pd(SR_1)_{17}(SR_2)$ that was prepared by ligand exchange reaction. If the resolution could be improved further, the geometrical structure of the product could be controlled even at

the level of coordination isomers. Furthermore, the mechanism of the ligand exchange reaction[116,119,125–127] of this type of clusters can be understood by evaluating the relative ratio of the coordination isomers. The separation of $Au_{24}Pd(SR_1)_{18-x}(SR_2)_x$ clusters into each coordination isomer was then attempted.

Herein, we describe the results of the products obtained from the reaction between $Au_{24}Pd(SC_2H_4Ph)_{18}$ and $C_{12}H_{25}SH$. The ligand exchange reaction was initiated by stirring $Au_{24}Pd(SC_2H_4Ph)_{18}$ and $C_{12}H_{25}SH$ (concentration ratio of 1:50) in dichloromethane for 4 min. Fig. 14a shows the MALDI mass spectra of the product. The mass spectra displayed peaks that could be attributed to $Au_{24}Pd(SC_2H_4Ph)_{18-x}(SC_{12}H_{25})_x$ (x = 0–7). Thus, this result indicated that the ligand exchange reaction took place under the experimental conditions employed.

The obtained product was then separated by RP-HPLC. A C18 column was used for this separation (Table 1). The product was first adsorbed onto the stationary phase as described in Section 4. Then, the products were eluted from the stationary phase in order of cluster surface polarity by transitioning of the mobile phase composition using a linear gradient program (Fig. 8). In the study of the previous section, methanol and tetrahydrofuran (THF) were used as the adsorption and elution solvents, respectively. In this study, acetonitrile and acetone were used as the adsorption and elution solvents instead of methanol and THF, respectively (Table 1). As a result, the peak corresponding to a cluster with a single chemical composition was separated into multiple peaks.[114]

Fig. 14b shows the chromatogram of the obtained products, which features a peak distribution similar to that in the MALDI mass spectrum. This shows that $Au_{24}Pd(SC_2H_4Ph)_{18-x}(SC_{12}H_{25})_x$ (x = 0–8) clusters was separated with high resolution depending on the ligand composition under the experimental conditions employed. Fig. 15 shows enlarged views of the group of peaks corresponding to $Au_{24}Pd(SC_2H_4Ph)_{18-x}(SC_{12}H_{25})_x$ (x = 0–5). $Au_{24}Pd(SC_2H_4Ph)_{18}$ displayed only one peak (Fig. 15a). $Au_{24}Pd(SC_2H_4Ph)_{17}(SC_{12}H_{25})$ displayed two peaks (Fig. 15b) and $Au_{24}Pd(SC_2H_4Ph)_{18-x}(SC_{12}H_{25})_x$ (x = 2–5) displayed multiple peaks (Fig. 15c–f). In the MALDI mass spectrum of each fraction in Fig. 15, only one peak corresponding to the single chemical composition of $Au_{24}Pd(SC_2H_4Ph)_{18-x}(SC_{12}H_{25})_x$ (x = 0–5) was observed, thus demonstrating that only clusters with the same chemical composition were present in the fractions of Fig. 15a–f. These results indicate that each coordination isomer of $Au_{24}Pd(SC_2H_4Ph)_{18-x}(SC_{12}H_{25})_x$ (x = 1–5) was separated with high resolution under the experimental conditions employed.

This separation allowed for a deeper understanding of the mechanism of ligand exchange reaction occurring in this type of the clusters. As shown in Fig. 15b, the chromatogram of $Au_{24}Pd(SC_2H_4Ph)_{17}(SC_{12}H_{25})$ displayed two peaks with retention times of 56.58 and 57.20 min. The calculated area ratio of these peaks obtained upon curve fitting of the peaks was 12:0.9 (Fig. 15b).

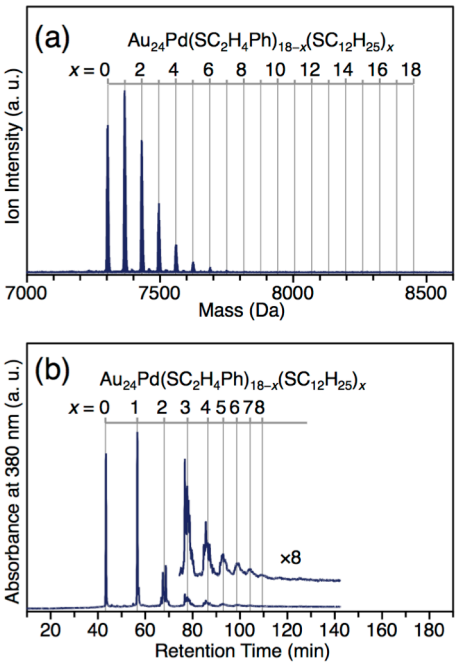

Fig. 14 Comparison between the (a) negative ion MALDI mass spectrum and (b) chromatogram obtained for $Au_{24}Pd(SC_2H_4Ph)_{18-x}(SC_{12}H_{25})_x$. Adapted from ref. 114.

This result indicates that the isomer distribution of the $Au_{24}Pd(SC_2H_4Ph)_{17}(SC_{12}H_{25})$ products was strongly biased. The peaks with retention times of 56.58 and 57.20 min were attributed to isomers exchanged at the core and apex sites, respectively (Fig. 15b).[114] This result implied that the first ligand exchange reaction occurred preferentially at the thiolate of the core site. A similar reaction preference was also observed in the second ligand exchange reaction.[114] Based on these results, it was concluded that the ligand exchange reaction is instigated by preferential reaction at thiolate bound at core sites in the reaction between $Au_{24}Pd(SC_2H_4Ph)_{18}$ and $C_{12}H_{25}SH$.[114] The results obtained in this study were also consistent with the interpretation of the reaction between $Au_{25}(SC_2H_4Ph)_{18}$ and *p*-bromobenzenethiol obtained by Ackerson and co-workers based on single-crystal X-ray structure analysis.[127] Häkkinen and co-workers performed density functional theory calculations on the ligand exchange reaction between $Au_{102}(SH)_{44}$ and CH_3SH, and proposed that such a reaction involves initial nucleophilic attack of S atom of CH_3SH on Au atom of a [–S(H)–Au–S(H)–] staple in $Au_{102}(SH)_{44}$.[119] The H atom of SH then bonds to S atom in the staple for the reaction to proceed. Also, $Au_{24}Pd(SC_2H_4Ph)_{18}$ has staples on its surface (Fig. 6). Thus, it can be considered that the reaction starts with a nucleophilic attack of the thiol on Au of the staple, even in the present system. However, in contrast to $Au_{102}(SH)_{44}$, the staples of the present system included two different S atoms that could be attacked by H of the thiol bound to Au, *i.e.*, one at the core site and the other at the apex site (Fig. 6). Our results showed that the attack of H of the thiol group

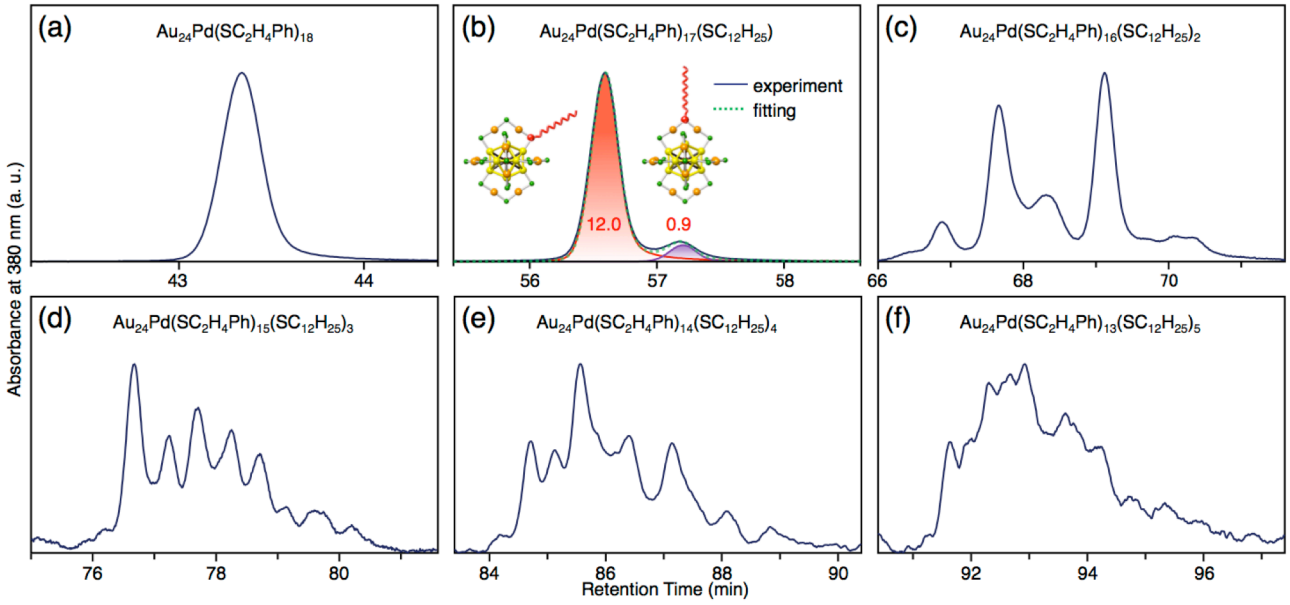

Fig. 15 Expanded chromatograms of (a) $Au_{24}Pd(SC_2H_4Ph)_{18}$, (b) $Au_{24}Pd(SC_2H_4Ph)_{17}(SC_{12}H_{25})$, (c) $Au_{24}Pd(SC_2H_4Ph)_{16}(SC_{12}H_{25})_2$, (d) $Au_{24}Pd(SC_2H_4Ph)_{15}(SC_{12}H_{25})_3$, (e) $Au_{24}Pd(SC_2H_4Ph)_{14}(SC_{12}H_{25})_4$, and (f) $Au_{24}Pd(SC_2H_4Ph)_{13}(SC_{12}H_{25})_5$. The fitting results are also shown in (b). The peak structure used for fitting is based on the peak structure of $Au_{24}Pd(SC_2H_4Ph)_{18}$ of (a) because the peak structure in the chromatogram does not show a symmetrical curve (see (a)). Adapted from ref. 114.

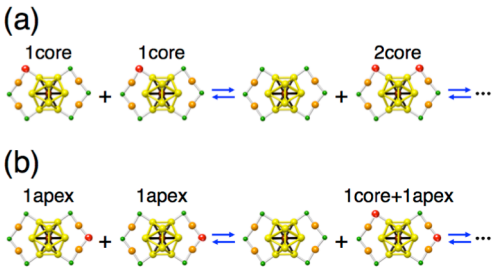

Scheme 1 Expected reactions (a) between two core-site type $Au_{24}Pd(SC_2H_4Ph)_{17}(SC_{12}H_{25})$ and (b) two apex-site type $Au_{24}Pd(SC_2H_4Ph)_{17}(SC_{12}H_{25})$ at the early stage of standing in solution. The isomer structures shown here are schematic illustrations only. Adapted from ref. 114.

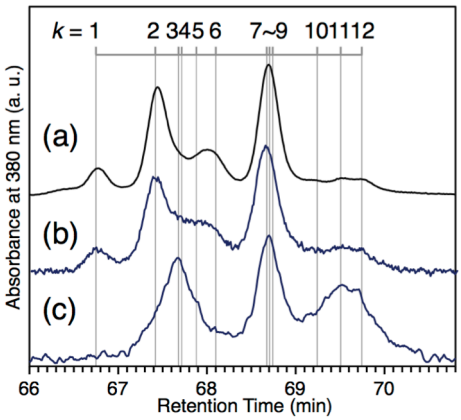

Fig. 16 Chromatograms of $Au_{24}Pd(SC_2H_4Ph)_{16}(SC_{12}H_{25})_2$ obtained by (a) reaction between $Au_{24}Pd(SC_2H_4Ph)_{18}$ and $C_{12}H_{25}SH$ in dichloromethane, (b) standing of core-site type $Au_{24}Pd(SC_2H_4Ph)_{17}(SC_{12}H_{25})$ in acetone, and (c) standing of apex-site type $Au_{24}Pd(SC_2H_4Ph)_{17}(SC_{12}H_{25})$ in acetone. Parameter *k* refers to isomer index used for tentative assignment of each isomer in ref. 114. Adapted from ref. 114.

on S occurred preferentially at the S of the core site on the [–S(R)–Au–S(R)–Au–S(R)–] (R = C_2H_4Ph) staples.[114]

It is worth noting that the ligand exchange reaction occurs even between the clusters.[120] Thus, when $Au_{24}Pd(SC_2H_4Ph)_{17}(SC_{12}H_{25})$ remains in solution, $Au_{24}Pd(SC_2H_4Ph)_{18}$ and $Au_{24}Pd(SC_2H_4Ph)_{16}(SC_{12}H_{25})_2$ form upon reaction of two $Au_{24}Pd(SC_2H_4Ph)_{17}(SC_{12}H_{25})$ (Scheme 1).[114] Based on the reaction mechanism (Scheme 1), the isomer distribution of $Au_{24}Pd(SC_2H_4Ph)_{16}(SC_{12}H_{25})_2$ generated by $Au_{24}Pd(SC_2H_4Ph)_{17}(SC_{12}H_{25})$ is expected to be different depending on the isomer structure of the precursor $Au_{24}Pd(SC_2H_4Ph)_{17}(SC_{12}H_{25})$. Our study using RP-HPLC revealed that the isomer distribution of the generated clusters is actually different depending on the coordination isomer distribution of the reactant clusters.[114] Fig. 16 shows chromatograms of $Au_{24}Pd(SC_2H_4Ph)_{16}(SC_{12}H_{25})_2$ generated after 0.5 h of standing in solution. The chromatogram of $Au_{24}Pd(SC_2H_4Ph)_{16}(SC_{12}H_{25})_2$ generated from a core-site isomer (Fig. 16b) was considerably different from that of $Au_{24}Pd(SC_2H_4Ph)_{16}(SC_{12}H_{25})_2$ generated from an apex-site isomer (Fig. 16c). Our tentative assignments of the peaks of $Au_{24}Pd(SC_2H_4Ph)_{16}(SC_{12}H_{25})_2$ revealed that the sample in Fig. 16b contained isomers with two $SC_{12}H_{25}$ at the core sites with a content of 71.6% as the main product, whereas the sample of Fig. 16c

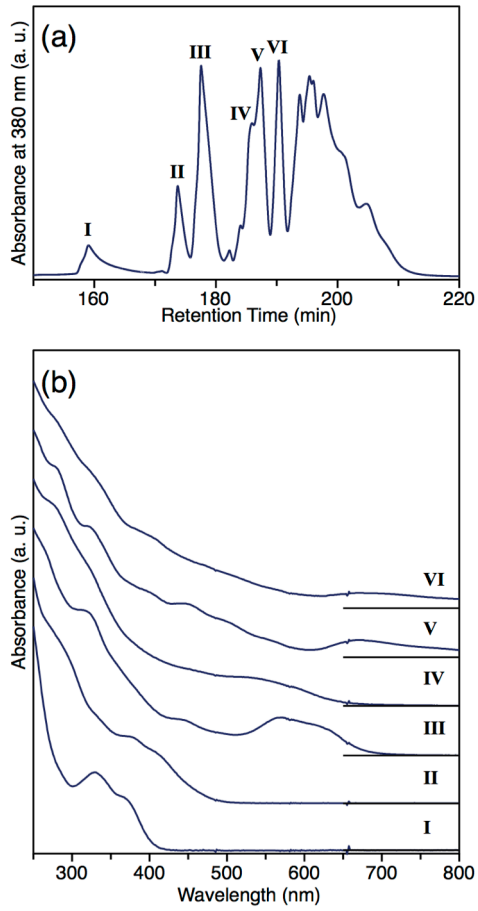

Fig. 17 (a) Chromatogram of a mixture of hydrophilic $Au_n(SG)_m$ clusters and (b) optical absorption spectra of the main peaks in (a).

contained isomers with one $SC_{12}H_{25}$ at the core site and one $SC_{12}H_{25}$ at the apex site with a content of 78.3% as the main product.[114] These results demonstrate that control of the coordination isomer distribution of the starting clusters enables control of the coordination isomer distribution of the products generated by ligand exchange reactions between clusters.

6. Separation depending on the core size for hydrophilic clusters

In the above discussed studies, hydrophobic clusters were used as the target materials for the high-resolution separation. On the other hand, hydrophilic clusters have also attracted much attention because they have a better affinity to biomaterials,[128–130] are very sensitive to toxic elements in aqueous solutions,[131,132] and exhibit photoluminescence properties with high quantum yields.[60,62] For the separation of such hydrophilic clusters, PAGE has been used as a powerful tool since the first report by Whetten and co-workers[73]. To date, clusters, such as $Au_{10}(SG)_{10}$, $Au_{15}(SG)_{13}$, $Au_{18}(SG)_{14}$, $Au_{22}(SG)_{16}$, $Au_{22}(SG)_{17}$, $Au_{25}(SG)_{18}$, $Au_{29}(SG)_{20}$, $Au_{33}(SG)_{22}$, and $Au_{39}(SG)_{24}$ (SG = glutathiolate), have been separated with high resolution using PAGE.[46] In this section, we describe that hydrophilic $Au_n(SG)_m$ clusters can also be separated by RP-HPLC.

In this study, $Au_n(SG)_m$ clusters were prepared by the method reported in the literature[46] and then the mixture was separated by RP-HPLC. A C18 column was used for the separation (Table 1). Mobile phase was transformed from 25 mM sodium phosphate buffer solution (pH 6.9) and 25 mM $TBAClO_4$ methanol solution using a linear gradient program (Table 1).

Fig. 17a shows the chromatogram of $Au_n(SG)_m$ clusters obtained. Multiple peaks were observed.[133] Fig. 17b shows the optical absorption spectra of the main peaks in Fig. 17a. The optical absorption spectrum of each peak was well consistent with that of $Au_{10}(SG)_{10}$ (I), $Au_{15}(SG)_{13}$ (II), $Au_{18}(SG)_{14}$ (III), $Au_{22}(SG)_{17}$ (IV), $Au_{25}(SG)_{18}$ (V), or $Au_{29}(SG)_{20}$ (VI), which has been previously separated by PAGE.[46] These results demonstrate that $Au_n(SG)_m$ clusters can also be separated by RP-HPLC. At present, RP-HPLC does not necessarily show a better resolution than PAGE. And the instrument employed for PAGE analysis is inexpensive. Thus, the cost for setting up the experimental system is rather inexpensive. Additionally, PAGE analysis enables visual examination of the color of the clusters and that of the photoluminescence emitted from the clusters. Therefore, we do not intend to say that RP-HPLC is superior to PAGE in the separation of hydrophilic clusters. However, the time required for the fractionation process is shorter in RP-HPLC (Fig. 17a) than in PAGE. Furthermore, RP-HPLC requires shorter times even for the recovery process of the separated clusters when compared with PAGE because RP-HPLC separation does not include time-consuming recovery processes such as gel cleaning, which is necessary in PAGE separation. Thus, RP-HPLC may be useful for the fractionation of clusters, of which the stability in solution is not so high. Other advantages of the RP-HPLC analysis include the high reproducibility of retention times. In the case that the absorption coefficient of each $Au_n(SR)_m$ is known, it is possible to evaluate the abundance ratio of each $Au_n(SR)_m$ cluster directly from the chromatogram. Moreover, RP-HPLC can be connected directly to an ESI mass spectrometer. These advantages render RP-HPLC one of the most powerful tools even for the separation of hydrophilic $Au_n(SR)_m$ clusters.

7. Future prospects

The above sections demonstrate that RP-HPLC has a high potential in the separation and analysis of thiolate-protected metal clusters. In this section, we describe the future prospects of RP-HPLC.

7.1. Study of other metal clusters

Thiolate-protected metal clusters comprising Ag,[134–144] Pd,[145] Pt,[146] and other metal elements exhibit different physical and chemical properties from those of $Au_n(SR)_m$ clusters. However, when compared with $Au_n(SR)_m$ clusters, fewer studies have been reported

on other metal clusters to date. The method described in Section 2 can be, in principle, applied to thiolate-protected metal clusters comprising other metal elements. It is thus expected that other metal clusters will also be systematically isolated by RP-HPLC and an in-depth understanding of the stable size and transition of the electronic/geometric structure will thus be obtained for other metal clusters in the future.

7.2. Separation of bimetallic clusters

Mixing different elements generates physical and chemical properties that are different from those of monometallic clusters.[147–149] Thus, the composition control of metal clusters is very interesting from the viewpoint of modification of the physical and chemical properties of clusters. Recently, it became possible to precisely synthesize bimetallic clusters.[12,40,113,143,150–155] However, there are various bimetallic clusters that are yet to be isolated with atomic precision. Examples of such clusters include $Au_{25-x}Ag_x(SR)_{18}$, $Au_{25-x}Cu_x(SR)_{18}$, $Au_{38-x}Ag_x(SR)_{24}$, $Au_{144-x}Ag_x(SR)_{60}$, and $Au_{144-x}Cu_x(SR)_{60}$, in which $Au_{25}(SR)_{18}$, $Au_{38}(SR)_{24}$, or $Au_{144}(SR)_{60}$ is doped with Ag or Cu.[109,113,156–165] Our recent study demonstrated that the retention time of clusters slightly varies depending on the degree of difference in the atomic radius or the charge state of the element near the metal core.[114] Thus, it is considered that separation of a series of the bimetal clusters will be achievable if the resolution can be improved further. It is expected that such a separation will be achieved and thereby the precise and systematic synthesis of those bimetal clusters will become possible.

7.3. Deepening the understanding of the interaction between the stationary phase and cluster surface

The separation shown in Fig. 2b was achieved by addition of $TBAClO_4$ to the mobile phase solvent. The improved separation in Sections 5 was achieved by changing the nature of the mobile phase solvent. In these studies, better conditions were established through repeated experiments. However, to achieve even higher resolution than the present resolution, deepening the understanding of the interactions between the stationary phase and cluster surface under those experimental conditions is important. If such an understanding is achieved, further optimized experimental conditions can be established for each separation, and thereby this type of metal clusters could be separated with higher resolution.

8. Concluding remarks

Our group has been studying the high-resolution separation of $Au_n(SR)_m$ clusters and their doped clusters using RP-HPLC. In this perspective, we summarized our recent results on the separation of those clusters according to the core size, charge state, ligand composition, and coordination isomer. The results obtained in our studies demonstrate that RP-HPLC has a high potential in the separation and analysis of thiolate-protected metal clusters. Furthermore, considering the availability of recently established variety of HPLC techniques, one can expect the development of additional other useful HPLC methods. As exemplified, Bürgi and co-workers recently demonstrated that HPLC using a chiral column is also useful for the separation of this type of metal clusters.[23,124,166–169] It is expected that numerous high-resolution separation methods will be established in the future, thereby affording the creation of $Au_n(SR)_m$ clusters with particular desired functional properties and functionalized nanomaterials based on such clusters.

Acknowledgments

The authors wishes to thank all the co-authors, especially Prof. Tatsuya Tsukuda (The University of Tokyo), Prof. Hannu Häkkinen (University of Jyväskylä), and Prof. Thalappil Pradeep (Indian Institute of Technology Madras). This work was supported by a Grant-in-Aid for Scientific Research on Innovative Areas “New Polymeric Materials Based on Element-Blocks (No. 2401)” (15H00763) of the Ministry of Education, Culture, Sports, Science, and Technology, Japan, the Canon Foundation, the Kajima Foundation, and the Nippon Sheet Foundation for Materials Science and Engineering. The first author expresses his gratitude towards the Sasagawa Foundation for partial financial support.

References

1. L. M. Liz-Marzan and P. V. Kamat in *Nanoscale Materials*, ed. L. M. Liz-Marzan and P. V. Kamat, Springer, Kluwer Academic Publishers, Boston, 2003. pp. 1-3.
2. M.-C. Daniel and D. Astruc, *Chem. Rev*., 2004, **104**, 293-346.
3. K. Ariga, A. Vinu, Y. Yamauchi, Q. Ji and J. P. Hill, *Bull. Chem. Soc. Jpn.*, 2012, **85**, 1-32.
4. M. Brust, M. Walker, D. Bethell, D. J. Schiffrin and R. Whyman, *J. Chem. Soc., Chem. Commun.,* 1994, 801-802.
5. T. Tsukuda, *Bull. Chem. Soc. Jpn.*, 2012, **85**, 151-168.
6. R. L. Whetten, M. N. Shafigullin, J. T. Khoury, T. G. Schaaff, I. Vezmar, M. M. Alvarez and A. Wilkinson, *Acc. Chem. Res.,* 1999, **32**, 397-406.
7. J. F. Parker, C. A. Fields-Zinna and R. W. Murray, *Acc. Chem. Res.,* 2010, **43**, 1289-1296.
8. R. W. Murray, *Chem. Rev.,* 2008, **108**, 2688-2720.
9. G. Li and R. Jin, *Acc. Chem. Res.*, 2013, **46**, 1749-1758.
10. H. Qian, M. Zhu, Z. Wu and R. Jin, *Acc. Chem. Res.,* 2012, **45**, 1470-1479.
11. A. Dass, *Nanoscale,* 2012, **4**, 2260-2263.
12. Y. Negishi, W. Kurashige, Y. Niihori and K. Nobusada, *Phys. Chem. Chem. Phys*., 2013, **15**, 18736-18751.
13. Y. Negishi, *Bull. Chem. Soc. Jpn.*, 2014, **87**, 375-389.
14. Z. Luo, V. Nachammai, B. Zhang, N. Yan, D. T. Leong, D.-e. Jiang and J. Xie, *J. Am. Chem. Soc.,* 2014, **136**, 10577-10580.
15. H. Häkkinen, *Nat. Chem.,* 2012, **4**, 443-455.
16. A. Fernando, K. L. D. M. Weerawardene, N. V. Karimova and C. M. Aikens, *Chem. Rev.*, 2015, **115**, 6112-6216.
17. A. Sánchez-Castillo, C. Noguez and I. L. Garzón, *J. Am. Chem. Soc*., 2010, **132**, 1504-1505.
18. Y. Pei and X. C. Zeng, *Nanoscale,* 2012, **4**, 4054-4072.
19. P. Zhang, *J. Phys. Chem. C*, 2014, **118**, 25291–25299.
20. D.-e. Jiang, M. Kühn, Q. Tang and F. Weigend, *J. Phys. Chem. Lett.*, 2014, **5**, 3286-3289.

21. P. D. Jadzinsky, G. Calero, C. J. Ackerson, D. A. Bushnell and R. D. Kornberg, *Science,* 2007, **318**, 430-433.
22. S. Knoppe, O. A. Wong, S. Malola, H. Häkkinen, T. Bürgi, T. Verbiest and C. J. Ackerson, *J. Am. Chem. Soc.,* 2014, **136**, 4129-4132.
23. I. Dolamic, S. Knoppe, A. Dass and T. Bürgi, *Nature Commun.,* 2012, **3**, 798-803.
24. T. Udayabhaskararao and T. Pradeep, *J. Phys. Chem. Lett.,* 2013, **4**, 1553-1564.
25. T. Dainese, S. Antonello, J. A. Gascón, F. Pan, N. V. Perera, M. Ruzzi, A. Venzo, A. Zoleo, K. Rissanen and F. Maran, *ACS Nano*, 2014, **8**, 3904-3912.
26. Y. Li, O. Zaluzhna and Y. Y. J. Tong, *Langmuir,* 2011, **27**, 7366-7370.
27. K. Kwak, S. S. Kumar, K. Pyo and D. Lee, *ACS Nano*, 2014, **8**, 671-679.
28. H. Yao, *J. Phys. Chem. Lett.,* 2012, **3**, 1701-1706.
29. H. Kouchi, H. Kawasaki and R. Arakawa, *Anal. Methods,* 2012, **4**, 3600-3603.
30. N. Sakai and T. Tatsuma, *Adv. Mater.,* 2010, **22**, 3185-3188.
31. P. J. G. Goulet and R. B. Lennox, *J. Am. Chem. Soc.,* 2010, **132**, 9582-9584.
32. A. Tlahuice-Flores, R. L. Whetten and M. Jose-Yacaman, *J. Phys. Chem. C*, 2013, **117,** 20867–20875.
33. O. Varnavski, G. Ramakrishna, J. Kim, D. Lee and T. Goodson, *J. Am. Chem. Soc.,* 2010, **132**, 16-17.
34. D. Bahena, N. Bhattarai, U. Santiago, A. Tlahuice, A. Ponce, S. B. H. Bach, B. Yoon, R. L. Whetten, U. Landman and M. Jose-Yacaman, *J. Phys. Chem. Lett.,* 2013, **4**, 975-981.
35. R. Philip, P. Chantharasupawong, H. Qian, R. Jin and J. Thomas, *Nano Lett.,* 2012, **12**, 4661-4667.
36. P. J. Krommenhoek, J. Wang, N. Hentz, A. C. Johnston-Peck, K. A. Kozek, G. Kalyuzhny and J. B. Tracy, *ACS Nano,* 2012, **6**, 4903-4911.
37. K. N. Swanick, M. Hesari, M. S. Workentin and Z. Ding, *J. Am. Chem. Soc.,* 2012, **134**, 15205-15208.
38. J. E. Matthiesen, D. Jose, C. M. Sorensen and K. J. Klabunde, *J. Am. Chem. Soc.,* 2012, **134**, 9376-9379.
39. Z. W. Wang, O. Toikkanen, B. M. Quinn and R. E. Palmer, *Small,* 2011, **7**, 1542-1545.
40. C. Yao, J. Chen, M.-B. Li, L. Liu, J. Yang and Z. Wu, *Nano Lett.*, 2015, **15**, 1281-1287.
41. M. Suda, N. Kameyama, M. Suzuki, N. Kawamura and Y. Einaga, *Angew. Chem., Int. Ed.*, 2008, **47**, 160–163.
42. J. Koivisto, S. Malola, C. Kumara, A. Dass, H. Häkkinen and M. Pettersson, *J. Phys. Chem. Lett.,* 2012, **3**, 3076-3080.
43. M. Zhu, H. Qian and R. Jin, *J. Phys. Chem. Lett.,* 2010, **1**, 1003-1007.
44. W. Chen and S. Chen, *Angew. Chem., Int. Ed.,* 2009, **48**, 4386-4389.
45. Z. Wu, D.-e. Jiang, A. K. P. Mann, D. R. Mullins, Z.-A. Qian, L. F. Allard, C. Zeng, R. Jin and S. H. Overbury, *J. Am. Chem. Soc.*, 2014, **136**, 6111-6122.
46. Y. Negishi, K. Nobusada and T. Tsukuda, *J. Am. Chem. Soc.,* 2005, **127**, 5261-5270.
47. Y. Negishi and T. Tsukuda, *J. Am. Chem. Soc.,* 2003, **125**, 4046-4047.
48. Y. Negishi, Y. Takasugi, S. Sato, H. Yao, K. Kimura and T. Tsukuda, *J. Am. Chem. Soc.,* 2004, **126**, 6518-6519.
49. T. P. Bigioni, R. L. Whetten and Ö. Dag, *J. Phys. Chem. B,* 2000, **104**, 6983-6986.
50. G. Ramakrishna, O. Varnavski, J. Kim, D. Lee and T. Goodson, *J. Am. Chem. Soc.,* 2008, **130**, 5032-5033.
51. S. Link, A. Beeby, S. FitzGerald, M. A. El-Sayed, T. G. Schaaff and R. L. Whetten, *J. Phys. Chem. B*, 2002, **106**, 3410-3415.
52. D. Lee, R. L. Donkers, G. Wang, A. S. Harper and R. W. Murray, *J. Am. Chem. Soc.*, 2004, **126**, 6193-6199.
53. G. Wang, T. Huang, R. W. Murray, L. Menard and R. G. Nuzzo, *J. Am. Chem. Soc.*, 2005, **127**, 812-813.
54. G. Wang, R. Guo, G. Kalyuzhny, J.-P. Choi and R. W. Murray, *J. Phys. Chem. B*, 2006, **110**, 20282-20289.
55. Z. Wu and R. Jin, *Nano Lett.*, 2010, **10**, 2568-2573.
56. C. Zeng, Y. Chen, G. Li and R. Jin, *Chem. Mater.*, 2014, **26**, 2635-2641.
57. E. S. Shibu, M. A. H. Muhammed, T. Tsukuda and T. Pradeep, *J. Phys. Chem. C,* 2008, **112**, 12168-12176.
58. S. A. Miller, J. M. Womick, J. F. Parker, R. W. Murray and A. M. Moran, *J. Phys. Chem. C,* 2009, **113**, 9440-9444.
59. S. Wang, X. Zhu, T. Cao and M. Zhu, *Nanoscale*, 2014, **6**, 5777-5781.
60. A. Ghosh, T. Udayabhaskararao and T. Pradeep, *J. Phys. Chem. Lett.*, 2012, **3**, 1997-2002.
61. J. Hassinen, P. Pulkkinen, E. Kalenius, T. Pradeep, H. Tenhu, H. Häkkinen and R. H. A. Ras, *J. Phys. Chem. Lett.*, 2014, **5**, 585-589.
62. Y. Yu, Z. Luo, D. M. Chevrier, D. T. Leong, P. Zhang, D.-e. Jiang and J. Xie, *J. Am. Chem. Soc.*, 2014, **136**, 1246-1249.
63. K. G. Stamplecoskie, Y.-S. Chen and P. V. Kamat, *J. Phys. Chem. C*, 2014, **118**, 1370-1376.
64. D. R. Kauffman, D. Alfonso, C. Matranga, H. Qian and R. Jin, *J. Am. Chem. Soc.*, 2012, **134**, 10237-10243.
65. M. Yu, C. Zhou, J. Liu, J. D. Hankins and J. Zheng, *J. Am. Chem. Soc.*, 2011, **133**, 11014-11017.
66. F. Aldeek, M. A. H. Muhammed, G. Palui, N. Zhan and H. Mattoussi, *ACS Nano*, 2013, **7**, 2509-2521.
67. C.-C. Huang, Z. Yang, K.-H. Lee and H.-T. Chang, *Angew. Chem., Int. Ed.*, 2007, **46**, 6824-6828.
68. P. Huang, G. Chen, Z. Jiang, R. Jin, Y. Zhu and Y. Sun, *Nanoscale*, 2013, **5**, 3668-3672.
69. X. Nie, C. Zeng, X. Ma, H. Qian, Q. Ge, H. Xu and R. Jin. *Nanoscale*, 2013, **5**, 5912-5918.
70. Y. Negishi, U. Kamimura, M. Ide and M. Hirayama, *Nanoscale*, 2012, **4**, 4263-4268.
71. Y. Li, O. Zaluzhna, B. Xu, Y. Gao, J. M. Modest and Y. Y. J. Tong, *J. Am. Chem. Soc.*, 2011, **133**, 2092-2095.
72. R. L. Whetten, J. T. Khoury, M. M. Alvarez, S. Murthy, I. Vezmar, Z. L. Wang, P. W. Stephens, C. L. Cleveland, W. D. Luedtke and U. Landman, *Adv. Mater.*, 1996, **8**, 428-433.
73. T. G. Schaaff, G. Knight, M. N. Shafigullin, R. F. Borkman and R. L. Whetten, *J. Phys. Chem. B*, 1998, **102**, 10643-10646.
74. T. G. Schaaff and R. L. Whetten, *J. Phys. Chem. B*, 2000, **104**, 2630-2641.
75. R. L. Wolfe and R. W. Murray, *Anal. Chem.*, 2006, **78**, 1167-1173.
76. M. M. F. Choi, A. D. Douglas and R. W. Murray, *Anal. Chem.*, 2006, **78**, 2779-2785.
77. R. L. Donkers, D. Lee and R. W. Murray, *Langmuir*, 2004, **20**, 1945-1952.
78. Y. Negishi, N. K. Chaki, Y. Shichibu, R. L. Whetten and T. Tsukuda, *J. Am. Chem. Soc.*, 2007, **129**, 11322-11323.
79. N. K. Chaki, Y. Negishi, H. Tsunoyama, Y. Shichibu and T. Tsukuda, *J. Am. Chem. Soc.*, 2008, **130**, 8608-8610.
80. Y. Shichibu, Y. Negishi, T. Tsukuda and T. Teranishi, *J. Am. Chem. Soc.*, 2005, **127**, 13464-13465.
81. H. Qian, Y. Zhu and R. Jin, *ACS Nano*, 2009, **3**, 3795-3803.
82. A. C. Dharmaratne, T. Krick and A. Dass, *J. Am. Chem. Soc.*, 2009, **131**, 13604-13605.
83. R. Jin, H. Qian, Z. Wu, Y. Zhu, M. Zhu, A. Mohanty and N. Garg, *J. Phys. Chem. Lett.*, 2010, **1**, 2903-2910.
84. Y. Yu, Z. Luo, Y. Yu, J. Y. Lee and J. Xie, *ACS Nano*, 2012, **6**, 7920-7927.
85. Y. Yu, X. Chen, Q. Yao, Y. Yu, N. Yan and J. Xie, *Chem. Mater.,* 2013, **25**, 946-952.
86. Y. Yu, Q. Yao, Z. Luo, X. Yuan, J. Y. Lee and J. Xie, *Nanoscale,* 2013, **5**, 4606-4620.
87. C. Zeng, Y. Chen, A. Das and R. Jin, *J. Phys. Chem. Lett.,* 2015, **6**, 2976-2986.
88. C. Zeng, H. Qian, T. Li, G. Li, N. L. Rosi, B. Yoon, R. N. Barnett, R. L. Whetten, U. Landman and R. Jin, *Angew. Chem., Int. Ed*., 2012, **51**, 13114-13118.
89. C. Zeng, C. Liu, Y. Pei and R. Jin, *ACS Nano,* 2013, **7**, 6138-6145.
90. C. Zeng, T. Li, A. Das, N. L. Rosi and R. Jin, *J. Am. Chem. Soc.,* 2013, **135**, 10011-10013.
91. P. R. Nimmala, S. Theivendran, G. Barcaro, L. Sementa, C. Kumara, V. R. Jupally, E. Apra, M. Stener, A. Fortunelli and A. Dass, *J. Phys. Chem. Lett.,* 2015, **6**, 2134-2139.
92. C. Zeng, Y. Chen, K. Kirschbaum, K. Appavoo, M. Y. Sfeir and R. Jin, *Sci. Adv.*, 2015, **1**, e1500045.
93. Z. Tang, D. A. Robinson, N. Bokossa, B. Xu, S. Wang and G. Wang, *J. Am. Chem. Soc.*, 2011, **133**, 16037-16044.
94. X. Yuan, B. Zhang, Z. Luo, Q. Yao, D. T. Leong, N. Yan and J. Xie, *Angew. Chem., Int. Ed.*, 2014, **53**, 4623-4627.
95. D. Zanchet, C. M. Micheel, W. J. Parak, D. Gerion and A. P. Alivisatos, *Nano Lett.*, 2001, **1**, 32-35.

96. C. J. Ackerson, P. D. Jadzinsky, G. J. Jensen and R. D. Kornberg, *J. Am. Chem. Soc.*, 2006, **128**, 2635-2640.
97. J. G. Worden, Q. Dai, A. W. Shaffer and Q. Huo, *Chem. Mater.*, 2004, **16**, 3746-3755.
98. T. P. Weber and P. W. Carr, *Anal. Chem*., 1990, **62**, 2620-2625.
99. E. L. Regalado, P. Zhuang, Y. Chen, A. A. Makarov, W. A. Schafer, N. McGachy and C. J. Welch, *Anal. Chem.*, 2014, **86**, 805-813
100. Y. Negishi, C. Sakamoto, T. Ohyama and T. Tsukuda, *J. Phys. Chem. Lett.*, 2012, **3**, 1624–1628.
101. Y. Negishi, T. Nakazaki, S. Malola, S. Takano, Y. Niihori, W. Kurashige, S. Yamazoe, T. Tsukuda and H. Häkkinen, *J. Am. Chem. Soc.*, 2015, **137**, 1206–1212.
102. M. S. Devadas, S. Bairu, H. Qian, E. Sinn, R. Jin and G. Ramakrishna, *J. Phys. Chem. Lett.*, 2011, **2**, 2752–2758.
103. M. S. Devadas, V. D. Thanthirige, S. Bairu, E. Sinn and G. Ramakrishna, *J. Phys. Chem. C*, 2013, **117**, 23155–23161.
104. H.-C. Weissker, H. B. Escobar, V. D. Thanthirige, K. Kwak, D. Lee, G. Ramakrishna, R. L. Whetten and X. López-Lozano, *Nat. Commun.*, 2014, **5**, 3785.
105. H. Qian, W. T. Eckenhoff, Y. Zhu, T. Pintauer and R. Jin, *J. Am. Chem. Soc.*, 2010, **132**, 8280–8281.
106. J. B. Tracy, G. Kalyuzhny, M. C. Crowe, R. Balasubramanian, J.-P. Choi and R. W. Murray, *J. Am. Chem. Soc.*, 2007, **129**, 6706–6707.
107. A. Dass, A. Stevenson, G. R. Dubay, J. B. Tracy and R. W. Murray, *J. Am. Chem. Soc.*, 2008, **130**, 5940–5946.
108. C. A. Fields-Zinna, R. Sardar, C. A. Beasley and R. W. Murray, *J. Am. Chem. Soc.*, 2009, **131**, 16266–16271.
109. Y. Negishi, T. Iwai and M. Ide, *Chem. Commun.*, 2010, **46**, 4713–4715.
110. Y. Negishi, W. Kurashige, Y. Niihori, T. Iwasa and K. Nobusada, *Phys. Chem. Chem. Phys.*, 2010, **12**, 6219–6225.
111. Y. Kim, R. C. Johnson and J. T. Hupp, *Nano Lett.*, 2001, **1**, 165–167.
112. Y. Negishi, W. Kurashige, Y. Kobayashi, S. Yamazoe, N. Kojima, M. Seto and T. Tsukuda, *J. Phys. Chem. Lett.*, 2013, **4**, 3579–3583.
113. W. Kurashige, Y. Niihori, S. Sharma and Y. Negishi, *J. Phys. Chem. Lett.*, 2014, **5**, 4134–4142.
114. Y. Niihori, Y. Kikuchi, A. Kato, M. Matsuzaki and Y. Negishi, *ACS Nano*, DOI: 10.1021/acsnano.5b03435.
115. Y. Niihori, M. Matsuzaki, T. Pradeep and Y. Negishi, *J. Am. Chem. Soc.*, 2013, **135**, 4946–4949.
116. R. Guo, Y. Song, G. Wang and R. W. Murray, *J. Am. Chem. Soc.*, 2005, **127**, 2752–2757.
117. V. R. Jupally, R. Kota, E. V. Dornshuld, D. L. Mattern, G. S. Tschumper, D.-e. Jiang and A. Dass, *J. Am. Chem. Soc.*, 2011, **133**, 20258–20266.
118. M. S. Devadas, K. Kwak, J.-W. Park, J.-H. Choi, C.-H. Jun, E. Sinn, G. Ramakrishna and D. Lee, *J. Phys. Chem. Lett.*, 2010, **1**, 1497–1503.
119. C. L. Heinecke, T. W. Ni, S. Malola, V. Mäkinen, O. A. Wong, H. Häkkinen and C. J. Ackerson, *J. Am. Chem. Soc.*, 2012, **134**, 13316–13322.
120. Y. Niihori, W. Kurashige, M. Matsuzaki and Y. Negishi, *Nanoscale*, 2013, **5**, 508–512.
121. Y. Niihori, M. Matsuzaki, C. Uchida and Y. Negishi, *Nanoscale*, 2014, **6**, 7889–7896.
122. Y. Negishi, W. Kurashige and U. Kamimura, *Langmuir*, 2011, **27**, 12289–12292.
123. W. Kurashige, S. Yamazoe, K. Kanehira, T. Tsukuda and Y. Negishi, *J. Phys. Chem. Lett.*, 2013, **4**, 3181–3185.
124. L.Beqa, D. Deschamps, S. Perrio, A.-C. Gaumont, S. Knoppe and T. Bürgi, *J. Phys. Chem. C*, 2013, **117**, 21619–21625.
125. M. J. Hostetler, A. C. Templeton and R. W. Murray, *Langmuir*, 1999, **15**, 3782–3789.
126. J. B. Tracy, M. C. Crowe, J. F. Parker, O. Hampe, C. A. Fields-Zinna, A. Dass and R. W. Murray, *J. Am. Chem. Soc.*, 2007, **129**, 16209–16215.
127. T. W. Ni, M. A. Tofanelli, B. D. Phillips and C. J. Ackerson, *Inorg. Chem.*, 2014, **53**, 6500–6502.
128. C.-A. J. Lin, T.-Y. Yang, C.-H. Lee, S. H. Huang, R. A. Sperling, M. Zanella, J. K. Li, J.-L. Shen, H.-H. Wang, H.-I Yeh, W. J. Parak and W. H. Chang, *ACS Nano*, 2009, **3**, 395–401.
129. C. J. Ackerson, M. T. Sykes and R. D. Kornberg, *Proc. Natl. Acad. Sci. U.S.A.*, 2005, **102**, 13383–13385.
130. Y. Levi-Kalisman, P. D. Jadzinsky, N. Kalisman, H. Tsunoyama, T. Tsukuda, D. A. Bushnell and R. D. Kornberg, *J. Am. Chem. Soc.*, 2011, **133**, 2976–2982.
131. Y.-H. Lin and W.-L. Tseng, *Anal. Chem.*, 2010, **82**, 9194–9200.
132. C.-C. Huang, Z. Yang, K.-H. Lee and H.-T. Chang, *Angew. Chem.*, 2007, **46**, 6824-6828.
133. Y. Niihori, C. Uchida, W. Kurashige and Y. Negishi, unpublished data.
134. Z. Wu, E. Lanni, W. Chen, M. E. Bier, D. Ly and R. Jin, *J. Am. Chem. Soc.*, 2009, **131**, 16672-16674.
135. T. U. B. Rao, B. Nataraju and T. Pradeep, *J. Am. Chem. Soc.*, 2010, **132**, 16304-16307.
136. I. Chakraborty, A. Govindarajan, J. Erusappan, A. Ghosh, T. Pradeep, B. Yoon, R. L. Whetten and U. Landman, *Nano Lett.*, 2012, **12**, 5861-5866.
137. F. Bertorelle, R. Hamouda, D. Rayane, M. Broyer, R. Antoine, P. Dugourd, L. Gell, A. Kulesza , R. Mitric and V. Bonacic-Koutecky, *Nanoscale*, 2013, **5**, 5637-5643.
138. J. Guo, S. Kumar, M. Bolan, A. Desireddy, T. P. Bigioni and W. P. Griffith, *Anal. Chem.*, 2012, **84**, 5304-5308.
139. O. M. Bakr, V. Amendola, C. M. Aikens, W. Wenseleers, R. Li, L. D. Negro, G. C. Schatz and F. Stellacci, *Angew. Chem., Int. Ed.*, 2009, **48**, 5921-5926.
140. L. G. AbdulHalim, N. Kothalawala, L. Sinatra, A. Dass and O. M. Bakr, *J. Am. Chem. Soc.*, 2014, **136**, 15865-15868.
141. M. S. Bootharaju, V. M. Burlakov, T. M. D. Besong, C. P. Joshi, L. G. AbdulHalim, D. M. Black, R. L. Whetten, A. Goriely and O. M. Bakr, *Chem. Mater.*, 2015, **27**, 4289-4297.
142. C. P. Joshi, M. S. Bootharaju and O. M. Bakr, *J. Phys. Chem. Lett.*, 2015, **6**, 3023-3035.
143. H. Yang, Y. Wang, H. Huang, L. Gell, L. Lehtovaara, S. Malola, H. Häkkinen and N. Zheng, *Nat. Commun.*, 2013, **4**, 2422.
144. Y. Negishi, R. Arai, Y. Niihori and T. Tsukuda, *Chem. Commun.*, 2011, **47**, 5693-5695.
145. D. J. Gavia and Y.-S. Shon, *ChemCatChem*., 2015, **7**, 892-900.
146. E. G. Castro, R. V. Salvatierra, W. H. Schreiner, M. M. Oliveira and A. J. G. Zarbin, *Chem. Mater.*, 2010, **22**, 360-370.
147. H. Zhang, T. Watanabe, M. Okumura, M. Haruta and N. Toshima, *Nat. Mater.*, 2012, **11**, 49-52.
148. K. Kusada, H. Kobayashi, R. Ikeda, Y. Kubota, M. Takata, S. Toh, T. Yamamoto, S. Matsumura, N. Sumi, K. Sato, K. Nagaoka and H. Kitagawa, *J. Am. Chem. Soc.*, 2014, **136**, 1864-1871.
149. K. Yamamoto, T. Imaoka, W.-J. Chun, O. Enoki, H. Katoh, M. Takenaga and A. Sonoi, *Nat. Chem.*, 2009, **1**, 397-402.
150. H. Qian, D.-e. Jiang, G. Li, C. Gayathri, A. Das, R. R. Gil and R. Jin, *J. Am. Chem. Soc.*, 2012, **134**, 16159-16162.
151. H. Yang, Y. Wang, J. Yan, X. Chen, X. Zhang, H. Häkkinen and N. Zheng, *J. Am. Chem. Soc*., 2014, **136**, 7197-7200.
152. S. R. Biltek, A. Sen, A. F. Pedicini, A. C. Reber and S. N. Khanna, *J. Phys. Chem. A*, 2014, **118**, 8314-8319.
153. S. R. Biltek, S. Mandal, A. Sen, A. C. Reber, A. F. Pedicini and S. N. Khanna, *J. Am. Chem. Soc.*, 2013, **135**, 26-29.
154. T. Udayabhaskararao, Y. Sun, N. Goswami, S. K. Pal, K. Balasubramanian and T. Pradeep, *Angew. Chem., Int. Ed.*, 2012, **51**, 2155-2159.
155. R. Jin and K. Nobusada, *Nano. Res.*, 2014, **7**, 285-300.
156. D. R. Kauffman, D. Alfonso, C. Matranga, H. Qian and R. Jin, *J. Phys. Chem. C*, 2013, **117**, 7914–7923.
157. X. Dou, X. Yuan, Q. Yao, Z. Luo, K. Zheng and J. Xie, *Chem. Commun.*, 2014, **50**, 7459–7462.
158. R. Kobayashi, Y. Nonoguchi, A. Sasaki and H. Yao, *J. Phys. Chem. C*, 2014, **118**, 15506–15515.
159. C. Kumara, C. M. Aikens and A. Dass, *J. Phys. Chem. Lett.*, 2014, **5**, 461–466.
160. Y. Negishi, K. Munakata, W. Ohgake and K. Nobusada, *J. Phys. Chem. Lett.*, 2012, **3**, 2209–2214.
161. E. Gottlieb, H. Qian and R. Jin, *Chem. Eur. J.*, 2013, **19**, 4238–4243.
162. C. Kumara and A. Dass, *Nanoscale*, 2012, **4**, 4084–4086.
163. C. Kumara and A. Dass, *Nanoscale*, 2011, **3**, 3064–3067.
164. A. C. Dharmaratne and A. Dass, *Chem. Commun.*, 2014, **50**, 1722–1724.
165. N. Bhattarai, D. M. Black, S. Boppidi, S. Khanal, D. Bahena, A. Tlahuice-Flores, S. B. H. Bach, R. L. Whetten and M. Jose-Yacaman, *J. Phys. Chem. C*, 2015, **119**, 10935–10942.

166. N. Barrabés, B. Zhang and T. Bürgi, *J. Am. Chem. Soc.*, 2014, **136**, 14361–14364.
167. B. Varnholt, I. Dolamic, S. Knoppe and T. Bürgi, *Nanoscale*, 2013, **5**, 9568–9571.
168. S. Knoppe, I. Dolamic, A. Dass and T. Bürgi, *Angew. Chem., Int. Ed.*, 2012, **51**, 7589–7591.
169. S. Knoppe and T. Bürgi, *Acc. Chem. Res.,* 2014, **47**, 1318–1326.